

LAMS-2570

CIC-14 REPORT COLLECTION  
**REPRODUCTION  
COPY**

**C.30**

**LOS ALAMOS SCIENTIFIC LABORATORY**  
**OF THE UNIVERSITY OF CALIFORNIA ○ LOS ALAMOS NEW MEXICO**

---

QUARTERLY STATUS REPORT OF THE LASL  
CONTROLLED THERMONUCLEAR RESEARCH PROGRAM  
FOR PERIOD ENDING MAY 20, 1961

LOS ALAMOS NATL LAB LIBS  
  
3 9338 00371 0414

## LEGAL NOTICE

This report was prepared as an account of Government sponsored work. Neither the United States, nor the Commission, nor any person acting on behalf of the Commission:

A. Makes any warranty or representation, expressed or implied, with respect to the accuracy, completeness, or usefulness of the information contained in this report, or that the use of any information, apparatus, method, or process disclosed in this report may not infringe privately owned rights; or

B. Assumes any liabilities with respect to the use of, or for damages resulting from the use of any information, apparatus, method, or process disclosed in this report.

As used in the above, "person acting on behalf of the Commission" includes any employee or contractor of the Commission, or employee of such contractor, to the extent that such employee or contractor of the Commission, or employee of such contractor prepares, disseminates, or provides access to, any information pursuant to his employment or contract with the Commission, or his employment with such contractor.

Printed in USA. Price \$.75. Available from the  
Office of Technical Services  
U. S. Department of Commerce  
Washington 25, D. C.

LAMS-2570  
CONTROLLED THERMONUCLEAR  
PROCESSES  
(TID-4500, 16th Ed.)

**LOS ALAMOS SCIENTIFIC LABORATORY**  
**OF THE UNIVERSITY OF CALIFORNIA LOS ALAMOS NEW MEXICO**

REPORT COMPILED: June 1961

REPORT DISTRIBUTED: June 30, 1961

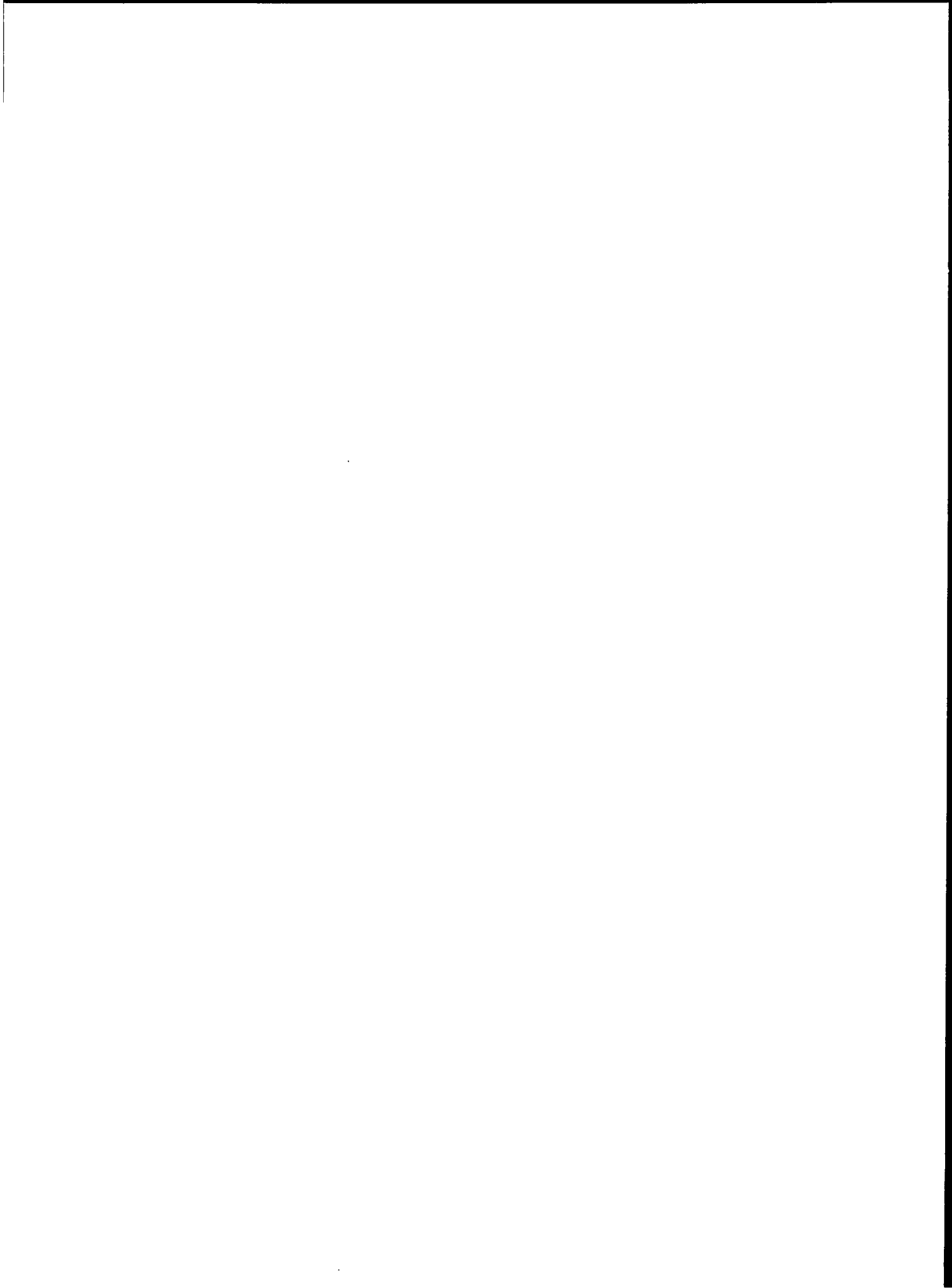
QUARTERLY STATUS REPORT OF THE LASL  
CONTROLLED THERMONUCLEAR RESEARCH PROGRAM  
FOR PERIOD ENDING MAY 20, 1961

Prepared from material submitted  
by members of P Division

Contract W-7405-ENG. 36 with the U. S. Atomic Energy Commission

All LAMS reports are informal documents, usually prepared for a special purpose. This LAMS report has been prepared, as the title indicates, to present the status of the LASL program for controlled thermonuclear research. It has not been reviewed or verified for accuracy in the interest of prompt distribution. All LAMS reports express the views of the authors as of the time they were written and do not necessarily reflect the opinions of the Los Alamos Scientific Laboratory or the final opinion of the authors on the subject.





## SUMMARY

1. The width of the He II 4686 Å line has been used to estimate the temperature of trapped helium ions injected into a simple picket fence magnetic field. With the assumption of a Maxwellian distribution, an average ion temperature of  $\sim 100$  eV is measured under optimum conditions in the interval 50-80  $\mu$ sec after the hydromagnetic gun is fired. This temperature is consistent with the energies of the injected ions. The electron energy has been measured by the ratio of the intensities of the He I 4921 Å and 4713 Å lines and found to be constant,  $\sim 20$  eV, between 50-80  $\mu$ sec. Significant amounts of contaminants from the gun electrodes are released which together with neutral gas diffusing from the hydromagnetic gun limit the lifetime of the particle density of the hot plasma to  $\sim 200$   $\mu$ sec.

2. The performance of the gun used in the bakeable picket fence experiment has been investigated as a function of center electrode polarity and method of switching. With the center electrode positive, the plasma ejected (measured by calorimeters 45 cm from the muzzle of the gun) is only  $\sim 8\%$  that when the electrode is negative. Ignitrons prove to be too resistive as switches with these fast guns and only  $\sim 25\%$  of the capacitor voltage appears across the gun terminals. Measurements of the neutron yield ( $\sim 5 \times 10^4$  per discharge) produced by the deuterium jet interacting with deuterium surface layers on a 10-cm diameter glass plate 45 cm from the gun are consistent with plasma jet densities of  $\sim 10^{13}$  deuterons/cm<sup>3</sup> and  $\sim 25$  keV energy.

3. A particle detector has been constructed which measures ion densities in plasma jets produced by fast hydromagnetic guns. Operating the gun at 28 kv, source capacity 2  $\mu\text{f}$ , ringing frequency 570 kc, plenum pressure 150 mm Hg, ion densities of  $10^{10}$  per  $\text{cm}^3$  with velocities  $\sim 2 \times 10^7$  at  $\sim 70$  cm from the gun muzzle are measured.

4. Perturbations of the feedpoint ( $\sim 3.7$  cm thick) of the one-turn coil on the magnetic field with the Orthogonal Pinch experiment have been studied by building a special symmetric coil fed by a parallel plate transmission line  $\sim 0.2$  cm thick. The neutron yield with the symmetric coil gave (unexpectedly) one-half the neutron yield with the thick feedpoint. Metal fins approximating a second feedpoint were attached to both coils with (1) a decrease in neutron yield of one-third with the thick feedpoint and (2) an increase in the neutron yield by only  $\sim 10\%$  for the symmetric coil. From these data it must be concluded that the mechanism of neutron production in this machine is influenced by the magnetic asymmetry introduced by the non-symmetric cross section of the driving coil geometry. The coil feedpoint also introduces electrostatic field perturbations early in the discharge cycle,  $\sim 12$  kv appearing across the feedpoint. Electrostatic shields placed on the glass discharge tube have shown that if these electrostatic field perturbations are important they are masked by magnetic field asymmetries.

5. In the resonant helix experiment the orbits of 2-kev electrons passing through the helix in the forward and backward directions have been followed by a computer for a number of longitudinal velocities of the electron. It is found that in the forward direction (the sense of rotation of the helix and orbiting particle the same) there is in general a step increase in the longitudinal energy. On several traversals of the helix these steps are accumulated until the mirror ratio is unable to contain the particle and it is lost. Containment times have been determined by measuring the diamagnetism produced by the trapped electrons and by the

loss rate of electrons out the far mirror. With a  $\sim 40$  cm long helix, perturbing field 4-6 gauss at the entrance, only 15 to 30 traversals between the mirrors are obtained.

6. The problem of the collisional relaxation of a fast test charge moving through a gas of field electrons and ions has been described by the asymptotic form of the Fokker-Planck equation, and an analytic solution has been obtained. The results are used to study the production of a second peak in the velocity distribution function.

7. In the study of the scattering of microwaves by plasmas, work is continuing on the study of the incoherent scattering induced by external fields. In particular, steps have been taken to measure the impedance of the plasma at the driving frequency. Preparations are also under way to measure coherent scattering from a plasma column immersed in a magnetic field.

8. In the colliding plasma experiment the fast components are observed to interact and produce plasma at temperatures of 3 kev at particle densities of  $\sim 10^{14}$  per  $\text{cm}^3$ . The slow components interact with considerable conversion of longitudinal to random energy producing  $kT_{\perp} \sim 100$  ev and density  $\sim 10^{16}$  per  $\text{cm}^3$ . In both cases there is no evidence of collective interaction.

9. The plasma from a coaxial gun has been observed to penetrate a transverse magnetic field and to polarize as expected.

10. In Scylla III the plasma is observed to develop an  $m = 2$  flute instability with superimposed rotation of the plasma as a whole. The plasma tends to stabilize when the compression coil is lengthened. The rate of growth of the flute is slower than theory would predict, indicating perhaps the stabilizing influence of the finite ion Larmor radii.

11. New spectral lines of F VIII and F IX have been excited in Scylla I and classified. Line broadening measurements of the impurity lines in Scylla I give equivalent O, F, and Ne ion temperatures much larger than the deuteron temperature inferred from broadening of the d-d proton line. Apparently there is either (1) a turbulent component of velocity or (2) greater decoupling of heavy ions and deuterons than would be indicated by theory, coupled with independent heating of heavy and light ions.

12. A new magnetic compression experiment is being designed to excite plasma in long coils. It will use a 560 kjoule, 50 kv capacitor bank, power crowbarred by a 3 Mjoule, 20 kv bank.

13. The low-inductance cabled shelf of Zeus has generated interest in the use of the system as a power crowbar in a new Scylla experiment. It has been found that, although Zeus has always been positive, parts should be charged negative. The negative polarity has required a change in the geometry of the switch header. The resulting coaxial header has a number of convenient features, including inherent low inductance, simplicity of construction, assembly and maintenance, use of a single ignitron to trigger all 16 load ignitrons, and no firing set capacitor.

### A. CAULKED PICKET FENCE

With the gun injecting a helium plasma into the picket fence magnetic field on the half-scale model, the energies of trapped ions were studied by means of Doppler broadening. The pertinent results are given in Table I. From this it is seen that between 50 and 80  $\mu$ sec the average ion energy is  $\sim 100$  ev; this is in satisfactory agreement with the average injected energy which lies between 100 and 160 ev. Further, when a probe is inserted, this energy is greatly reduced irrespective of whether the probe is seen directly by the monochromator or not. A check on this type of measurement is obtained by filling the tank with sufficient helium to provide appreciable charge exchange in the times of interest; the observed energy decreases as it should.

The electron temperature was deduced from the ratio of intensities of two neutral helium lines. At 50  $\mu$ sec this was  $\sim 20$  ev and then dropped at  $\sim 6$  ev/100  $\mu$ sec (measured values were obtained between 50 and 140  $\mu$ sec). This low an electron temperature allows field intermixing in  $\sim 25$   $\mu$ sec, which explains the disappearance of high- $\beta$  signals after 30  $\mu$ sec. The electrons must also be cooled by some energy loss process since after the field intermixing takes place they should have a temperature equal to half that of the ion energy.

The lifetime of the ions may be estimated from the intensity decay of the ionic light. The result is an exponential lifetime of  $\sim 200$   $\mu$ sec. This is approximately equal to that expected from charge exchange with the neutral gas, emitted by the gun before firing, diffusing into the confinement region.

Significant amounts of contaminants are released by the gun since their light intensity is of the same order as that of the injected gas. In an effort to reduce these contaminants the half-scale tank is to be used as a drift tube in conjunction with the full-scale apparatus.

TABLE I

Average ion energies as deduced from the width of the singly ionized helium line at 4686 Å.

<u>Conditions</u>	<u>Time (<math>\mu</math>sec)</u>	<u>Average Ion Energy (ev)</u>
Cusp field 430 gauss (all cases)	50	80
Base pressure $3-6 \times 10^{-6}$ mm Hg.	60	115
	70	105
	80	90
Base pressure $3-6 \times 10^{-6}$ mm Hg.	50	50
Probe inserted to $z = 0$	60	65
	70	50
	80	35
Base pressure $3-6 \times 10^{-6}$ mm Hg.	50	60
Probe inserted to $z = 10$	60	40
(out of direct view of monochromator)	70	35
	80	35
Helium admitted to system to	50	50
raise base pressure to $8 \times 10^{-5}$ mm Hg	60	35
	70	55
	80	45

## B. BAKEABLE PICKET FENCE (MARK II)

The Mark II bakeable picket fence has been received from the manufacturer and its installation has been completed. Initial experiments have been performed without baking as the vacuum chamber has been temporarily assembled with Neoprene gaskets. Experimental work to date has been largely confined to optimizing the performance of the plasma gun firing into this picket fence geometry. The gun used in this experiment is of the short, high-speed, coaxial type, previously described, and is operated at low gas loads. In an effort to optimize the gun to produce higher plasma densities than in previous experiments, the condensers were installed to allow use of ignitrons and higher gas loads. Previous experiments were limited in the gas loads used by the ability of the gun to hold off the condenser voltage until switched by a spark plug -- the so-called "switchless" operation. It was immediately found, however, that ignitrons are characteristically too resistive during the first  $\sim 1/2$   $\mu$ sec after firing to be used with the high-speed gun circuit as almost all of the useful acceleration takes place during this period. Similar experiments using spark gaps are being planned to circumvent the difficulty.

The performance of the "switchless" gun was then checked for both positive and negative polarity of the central electrode. Briefly, positive polarity gave only  $\sim 8\%$  of the total calorimetric output observed for the usual negative polarity operation. This marked difference in operation is as yet not understood although electrode markings indicate that the positive discharge broke up at approximately the location of the gas ports and did not propagate on toward the gun muzzle.

The performance of the "switchless" gun operated with a negative central electrode polarity, with 4  $\mu\text{f}$  charged to 24 kv, 125 mm.Hg plenum pressure, and 340  $\mu\text{sec}$  gas delay, is such as to yield an output of  $\sim 10$  joules in a 4-in. diameter calorimeter located 45 cm from the gun muzzle. This plasma jet produces  $\sim 5 \times 10^4$  neutrons on striking a 4-in. diameter Pyrex plate, which has molecular layers of deuterium on its surface and is loaded by previous discharges, located 100 cm from the gun muzzle. These preliminary measurements are consistent with a plasma jet which contains a density of  $\sim 10^{13}$  deuterons/ $\text{cm}^3$  with an energy of  $\sim 25$  kev. Very preliminary measurements of this plasma in the picket fence magnet show that the jet is capable of producing a high- $\beta$  region in fields of up to  $\sim 2$  kgauss with a  $\sim 40$   $\mu\text{sec}$  mean decay time of the diamagnetic signal. More detailed measurements of the diamagnetic signals will be undertaken when installation of a second gun is completed to permit the use of colliding plasmas.

### C. HYDROMAGNETIC GUN OPERATION

A fast hydromagnetic coaxial gun has been set up to study the plasma ejected when run at low gas pressures, low source inductance, and

relatively high voltages and currents. Three diagnostic techniques were used: calorimeter-thermocouple, magnetic probe, and single particle detector.

Parameters characteristic of the experiment were:

Capacity	2 $\mu$ fd
Voltage	28 kv
Gun frequency	570 kc
Total inductance of gun	$3.9 \times 10^{-8}$ henry
Peak Current	200 ka
Plenum pressure (deuterium)	150-400 mm Hg
Gas pressure between electrodes at firing time	20 $\mu$ Hg
Energy in plasma jet	5 joules

Measurements of the time-space history of the distribution of neutral gas pulsed in between the electrodes from the plenum were made with a CK 5702 subminiature pentode modified as an ion gage. As expected, no gas appeared until 150  $\mu$ sec after the fast electromagnetic valve was energized. The spatial distribution showed a peak density over the inlet holes between 250  $\mu$ sec and 400  $\mu$ sec, at which time a uniform diffusion along the electrodes set in. For this experiment the machine was fired by spark plugs when the gas density was sharply peaked over the inlet holes of the center electrode.

The firing time of the gun was then optimized against a thermocouple calorimeter situated 30 cm downstream from the gun muzzle, in a 1-meter long, 1-meter diameter tank. The base pressure in the tank was  $10^{-6}$  mm Hg. Reduction of the peak 5-joule output of the gun occurred when the spark plugs were fired early before enough gas was available or when they were fired late, after the gas reached a uniform distribution along the barrel.

A positive ion detector was developed as shown in Fig. 1, which operates successfully up to particle densities of  $10^{11}$  ions/cm<sup>3</sup>. The principle of operation is as follows: the external metal container floats at plasma potential and shields a bias electrode and a collector plate.

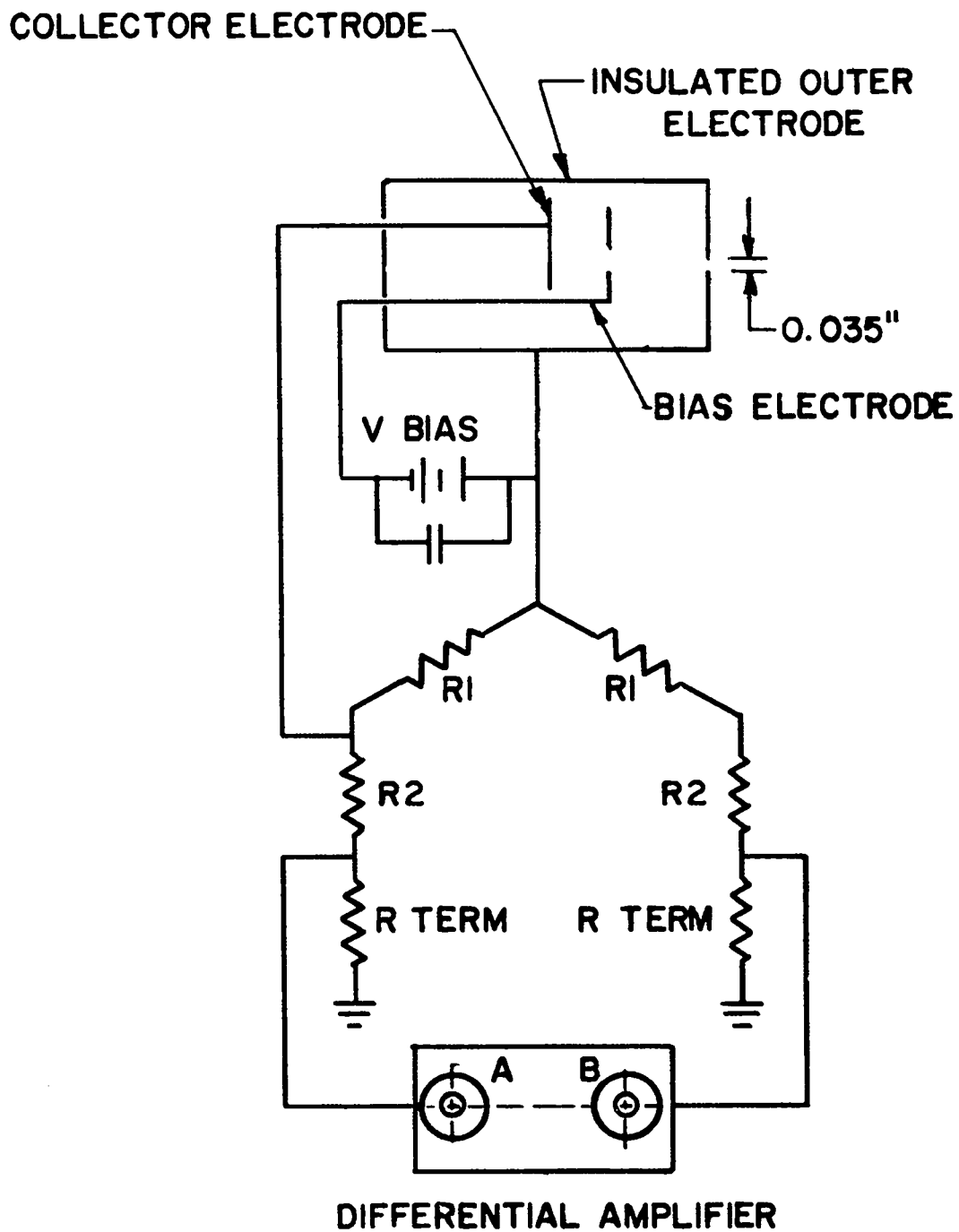


Fig. 1. Positive ion detector circuit

A bias voltage of 900 v is sufficient to repel incoming electrons and a 50-gauss magnetic field between the collector and bias electrodes suppresses any secondary electrons from the collector. Connected to a bridge circuit as shown, the plasma potential at the detector during the pulse is cancelled out. Ion currents are measured to the collector and are related to the plasma density by

$$I = n e v A$$

where  $n$  is the number of ions,  $e$  the charge,  $v$  the ion velocity, and  $A$  the area of the entrance aperture. A dual-beam scope picture (1 cm/ $\mu$ sec) is seen in Fig. 2. The upper trace is gun current as detected by a probe 2 cm downstream from the muzzle; the ion current signal is shown below.

Ion velocities of about  $3 \times 10^7$  cm/sec were measured from the time of flight. Velocity components considerably higher than this were obscured by noise resulting from shocks exciting the bridge circuit which is balanced to no better than 3% at 10 Mc.

In the case of 150-mm plenum pressure, ion densities of about  $10^{10}$  per  $\text{cm}^3$  were found on the axis 70 cm from the muzzle of the gun. This is to be compared with a peak gas density at firing time of  $\sim 5 \times 10^{14}$  per  $\text{cm}^3$ .

#### D. ORTHOGONAL PINCH

It has been found that the angular distribution of the axial magnetic field produced by a single-turn mirror coil (mirror ratio 1.02:1) is not azimuthally symmetric in the mirror region. A polar distribution of the  $B_z$  field measured near the inner surface of the coil shows a gradual reduction of the field as the feedpoint is approached. The feedpoint connections in this case are approximately 3.7 cm thick and begin to perturb the angular distribution at angles of  $\pm 90^\circ$  from the feedpoint; at the feedpoint, the  $B_z$  field is  $\sim 7.5\%$  lower than that at a point  $180^\circ$  away.

In order to examine the effects of this field asymmetry on neutron production, a special coil was constructed in which the feedpoint thickness

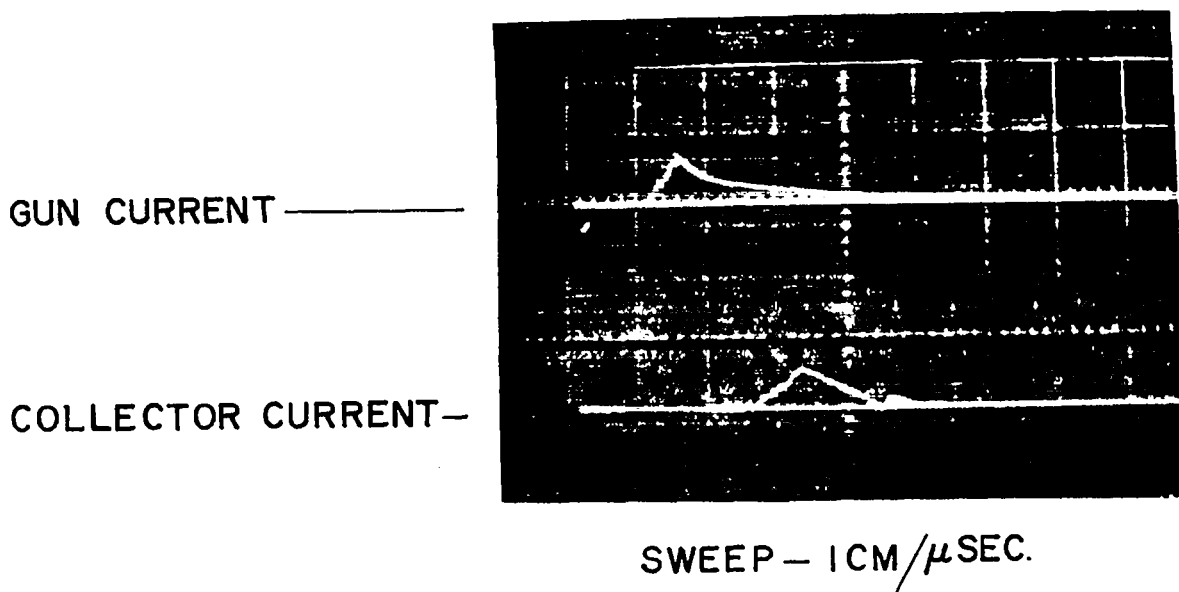


Fig. 2. Gun current and ion current observed with positive ion detector

was reduced to 0.2 cm -- this is called the symmetric coil. In comparison with the massive asymmetric coil, the optimum neutron yield from the symmetric geometry was reduced a factor of two. This result gave the first evidence that neutron production was enhanced by an asymmetric magnetic field.

By attaching a radial metal fin (3 x 20 x 30 cm) along the length of the massive coil, simulating a second massive feedpoint connection, the distribution of the  $B_z$  field in the mirror region was made more symmetric when the metal fin was located  $180^\circ$  from the real current feedpoint. The neutron yield with the attached fin was reduced a factor of 3 in comparison with no metal fin. This again indicated the importance of an annular asymmetry in the  $B_z$  field in terms of neutron production.

The same metal fins were also attached to the symmetric coil at various angles. The result shows that the attachment of one fin increased the neutron yield by  $\sim 10\%$  while the addition of a second fin reduced the yield  $10\%$ . A polar plot of the  $B_z$  field for the symmetric coil has not been made.

For the massive coil, the asymmetry in the  $B_z$  field becomes negligible as the midplane of the coil is approached. This result together with the neutron effects suggest that the mirror region contributes to the neutron yield or that the mechanism responsible for neutron production is enhanced by the angular asymmetry of the axial field. Even though the formation and detachment of the current sheath at the inner surface of the tube walls and the subsequent contraction to form a plasma take place rapidly -- in fact the time of contraction is generally much less than that for an appreciable change in primary current -- the effects of small magnetic asymmetries can be expected to influence or govern the starting conditions of the pinch. The result of small field asymmetries may initiate the onset of magnetic field intermixing observed with magnetic probes, causing plasma heating and finally neutron production.

The effect of an electrostatic potential at the current feedpoint in the orthogonal pinch geometry was investigated. A metallic shield covering

one half of the discharge tube and spanning the feedpoint and which could be rotated in situ produced no observable change in the neutron yield. The magnetic effect discussed earlier may have masked the electrostatic effect; this will be reinvestigated with the symmetric coil.

#### E. RESONANT HELIX

The containment time of electrons injected into the resonant helix apparatus has been investigated in three different ways. These different approaches give consistent answers and allow certain conclusions to be drawn concerning the success of the device to trap and contain particles.

The first approach is to investigate perturbations of the magnetic moment of the particle as it passes through the helix under different initial conditions. Measurement of this effect has been completed both theoretically and experimentally. The IBM 704 code used previously to check the resonance conditions was used to calculate changes in the longitudinal velocity confinements of the 2-keV particle with initial axial energies of 1.75, 1.50, 1.25, 1.00, 0.75, 0.50, and 0.25 keV after one transit of the helix. For each of these axial energies four phases were chosen  $90^\circ$  apart for the particle entering the helix. Typical computer results for a 3-meter long helix operating in a 100-gauss axial field are shown in Fig. 3.

Examination of this figure shows the mechanism for the principal loss of particles from the helix. In the interval 0 to 180 cm at the entrance of the helix the particle alternately is accelerated and decelerated by the perturbing field, producing a modulation in the longitudinal velocity analogous to beats occurring in a two-frequency system of harmonic oscillators. However, as the longitudinal velocity matches the spacing of the helix coils, a large step takes place in the velocity. It has been shown by analyzing many computer runs and also by statistical arguments that this step takes place predominantly in such a direction as to lose particles from the machine, i.e., to decrease the magnetic moment. This is the major

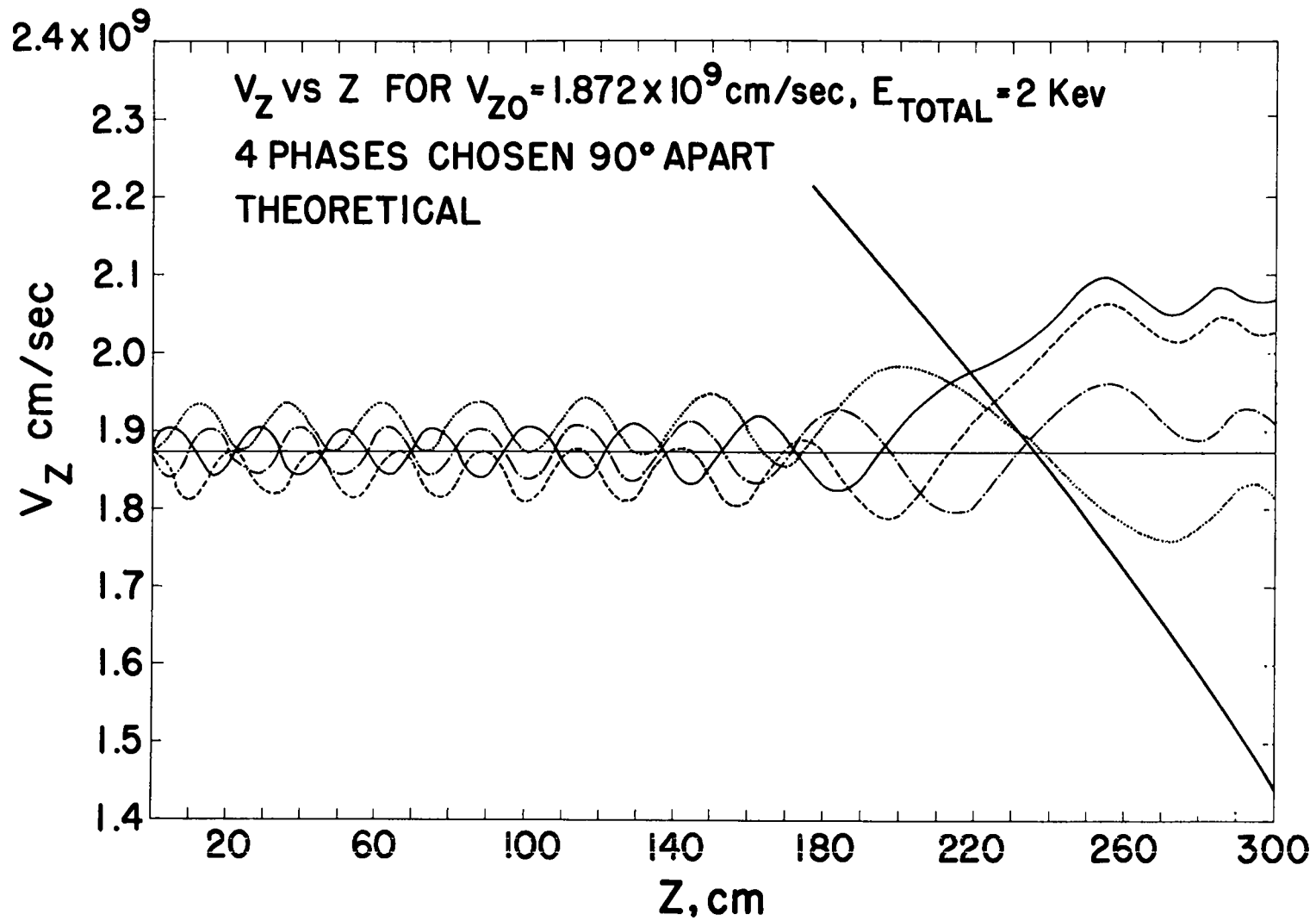


Fig. 3. Calculated longitudinal velocities of 2-keV particle as function of distance

loss process from the device. The size of the step appears to vary inversely as the square root of the length of the helix

$$v_z \propto L^{-1/2},$$

whereas the beat amplitude varies as the inverse of the length. If a random walk loss process is assumed, the loss rate varies as the square of the step size. It appears from these results that lengthening the helix may not be sufficient to contain particles for times of interest.

The step and its size have been confirmed experimentally using the electron analogue experiment described in the last quarterly report (LAMS-2529). For these experiments two helices were used in tandem, the first to put some energy in the perpendicular direction, and the second simulating the third pass through the apparatus. The Larmor radii were measured utilizing a fluorescent screen. The phase of the input particles was changed by varying the spacing between the two helices. From these data the perturbation of the magnetic moment could be determined. The results of the experiments are shown in Fig. 4. These results may be compared with the theoretical values shown in Fig. 5. The agreement is good and when a random walk calculation is made on the data it indicates particle containment for about 15 traversals of the system.

The second measurement of containment time was done by observing the diamagnetic signal produced by the trapped electrons. For this experiment the beam was modulated at a frequency of 35 cps and the signal from a 3000-turn coil was detected by means of a narrow band lock-in amplifier. The signal is proportional to the change in the magnetic field strength inside the pickup coil due to the trapped particles, and is a measure of the number of particles circulating within the system in equilibrium conditions. As the radius and pitch of the Larmor spiral of the trapped particles are not constant before particles are lost, the change in signal between one pass of the beam through the helix (no mirror current) and that produced with mirrors on does not give the increased number of traversals but a lower limit to the number of traversals a particle may make

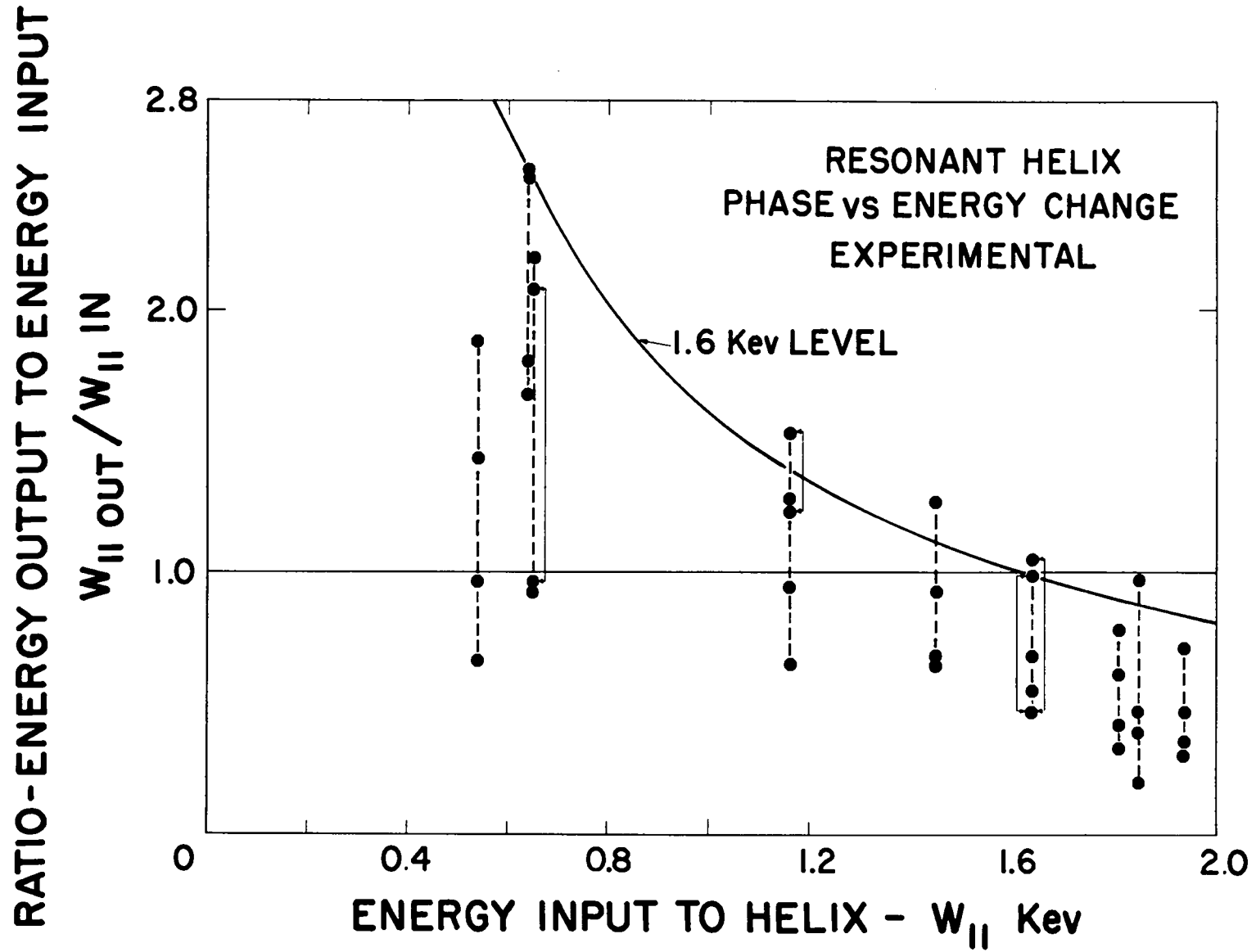


Fig. 4. Experimental values of perturbation of magnetic moment in resonant helix

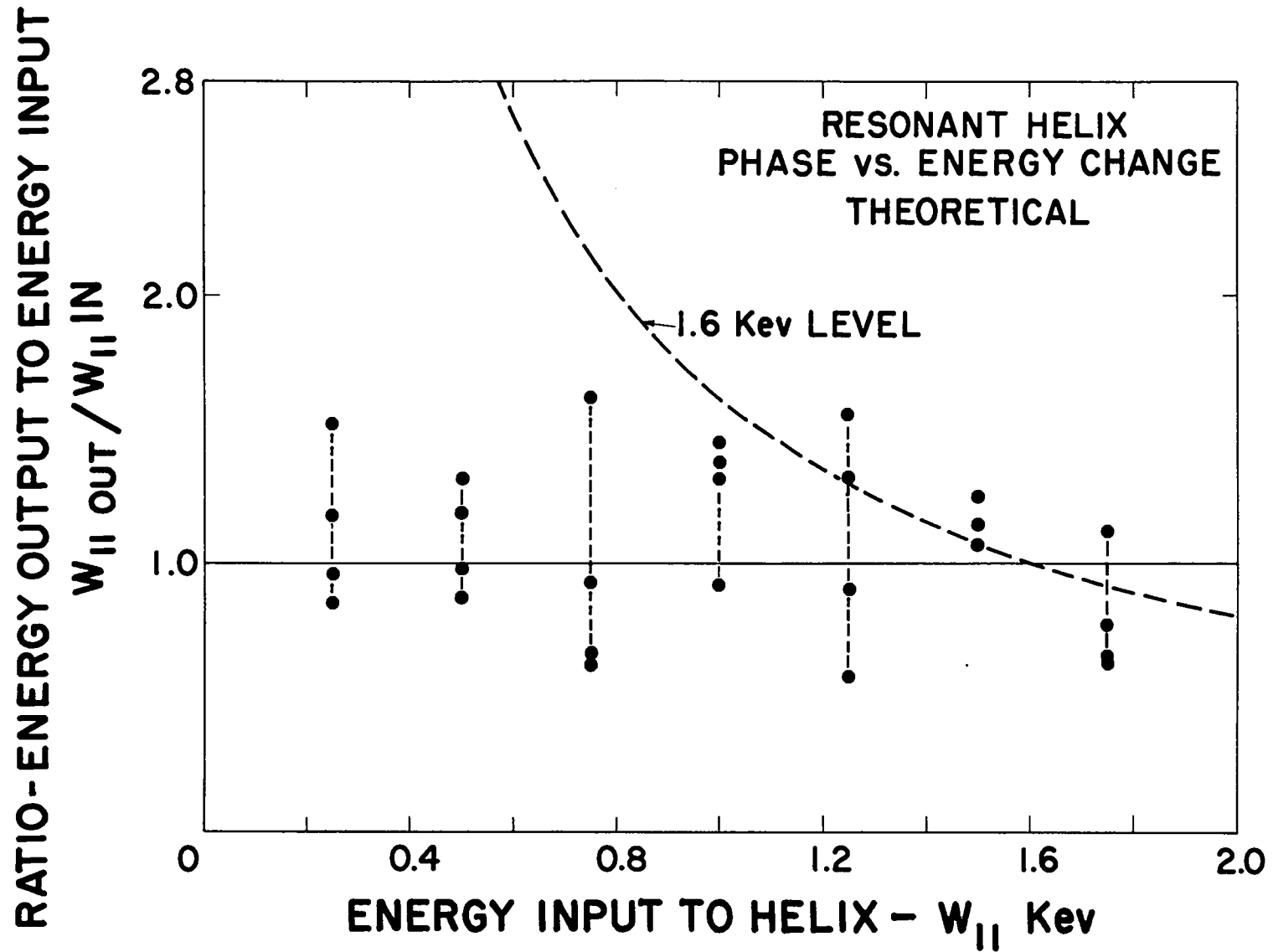


Fig. 5. Theoretical values of perturbation of magnetic moment in resonant helix

before being lost from the system. The results of this experiment give an increase by a factor of about 10 in magnetic signal between one traversal of the beam and the contained electrons. This corresponds to 15 to 30 traversals between the mirrors.

The decay of the current collected outside the far mirror (where most losses occur) has also been measured and indicates a confinement time of  $\sim 2 \mu\text{sec}$ , corresponding to about 15 reflections on the average. Oscillograms of this decay are shown in Fig. 6. This decay is not a simple exponential, however, and exhibits a long tail which has not been explained as yet.

In summary, it has been learned that the resonant helix system will trap particles, but is quite leaky owing to the same mechanism which achieves the trapping. It does not appear profitable to increase the confinement time by lengthening the helix, since the time varies only inversely as the length. Some possibility exists for increasing the confinement by dissociation of molecular ions within the device, thus removing the region of resonance between the helix and the orbiting particle. Calculations show this probably would not increase confinement time sufficiently to be of thermonuclear interest. However, in this case confinement time varies inversely as the square of the length and a density of  $10^{11}$  particles/cm<sup>3</sup> might be feasible. Pulsed operation of the device is being considered as a possible alternative.

A design for a resonant helix has been calculated based on more realistic assumptions than were reported in the preceding quarterly report (IAMS-2529, p. 20). Start with the vector equation of motion

$$\frac{d\vec{v}}{dt} = \frac{e}{mc} \vec{v} \times \vec{B} \quad (1)$$

and assume that

- (1)  $B_z$ , the axial component of the magnetic field, is constant.
- (2)  $B_r$ , the magnitude of the perturbing transverse field, and  $\psi$ , its azimuthal direction, are functions of  $z$  only.

ELECTRON CONFINEMENT IN MAGNETIC MIRROR WITH  
RESONANT HELIX INJECTION VS. HELIX CURRENT

$R_m = 3.4$   $B_0 = 90$  GAUSS  $E_e = 2.1$  KEV.  $I = 40 \mu A$

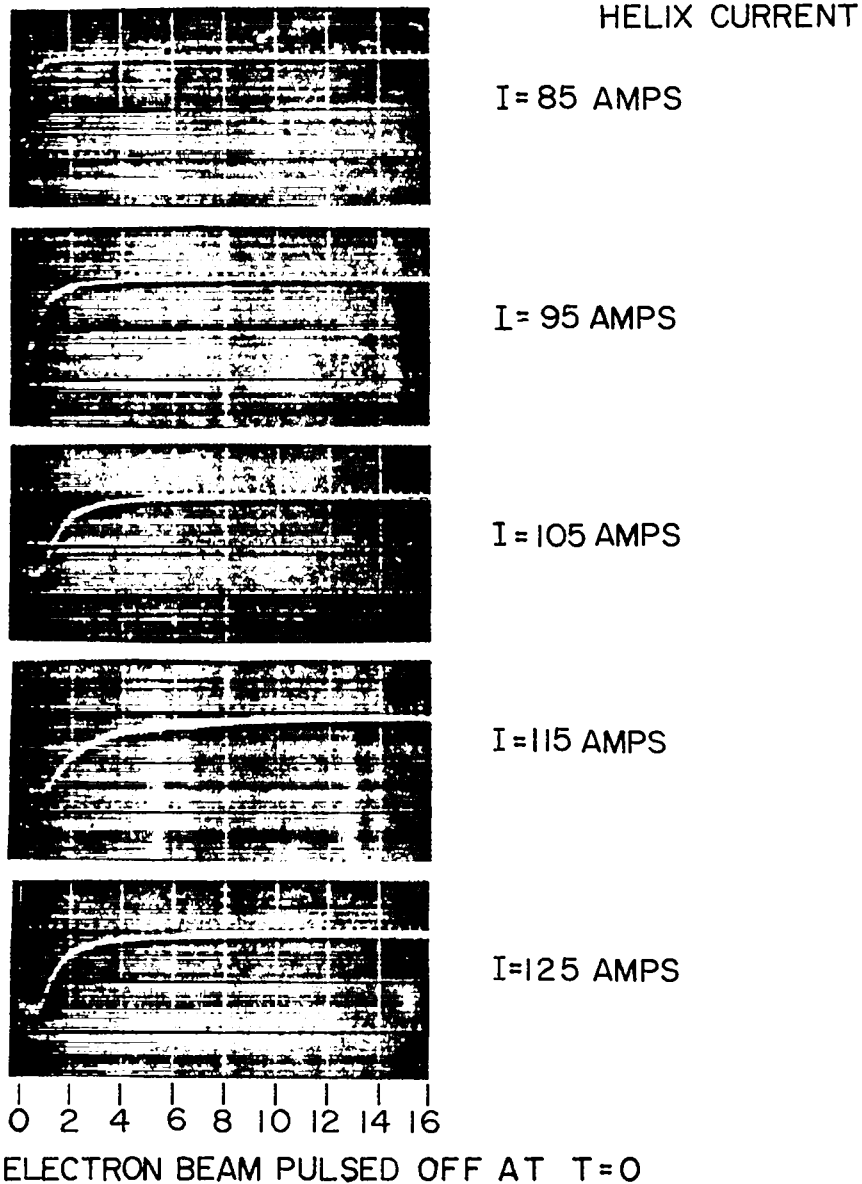


Fig. 6. Decay of current collected outside the far mirror from a resonant helix system

Let  $\theta$  be the angle between the z-direction and the particle velocity,  
 $\phi$  be the azimuthal angle of the velocity and  
 $v_0$  be the constant speed of the particle.

Then for any  $B_r$  and  $\psi$ ,

$$\frac{d}{dz} \sin \theta = \frac{e}{mcv_0} B_r \sin (\phi - \psi) \quad (2)$$

$$\frac{d}{dz} (\phi - \psi) = \frac{d\psi}{dz} - \frac{e}{mcv_0} \left[ \frac{B_z}{\cos \theta} - \frac{B_r \cos (\phi - \psi)}{\sin \theta} \right]. \quad (3)$$

From equations (2) and (3) the orbit of the particle can be calculated starting with any given initial values of  $\theta$  and  $\phi$  once  $B_r$  and  $\psi$  are known as functions of  $z$ .

If the particle orbit is exactly in resonance with the magnetic field the velocity is always perpendicular to the field direction and

$$\phi - \psi = 90^\circ. \quad (4)$$

Then  $\theta$  and  $\psi$  can be eliminated and equations (2) and (3) solved for the transverse field strength in terms of the rate of change of its azimuth (or pitch)

$$B_r = \frac{B_z \frac{d^2\psi}{dz^2}}{\left(\frac{d\psi}{dz}\right)^2 + \sqrt{\left(\frac{mcv_0}{eB_z} \cdot \frac{d\psi}{dz}\right)^2 - 1}}. \quad (5)$$

The relation between  $B_r$  and  $\frac{d}{dz}$  for an infinite helix of constant diameter and with constant pitch is a known function involving Bessel functions of complex arguments. Assuming, as an approximation, that the same relation between  $B_r$  and  $\psi$  holds for a helix of variable pitch, and using this relation together with equation (5), both  $B_r$  and  $\psi$  can be calculated as a function of  $z$  by numerical integration. The calculation has been carried

through for the case in which the radius of the helix is four times the Larmor radius of the resonant particle orbit in the  $B_z$  field, and of such a length that 75% of the total energy is changed from longitudinal to transverse energy.

#### F. ASYMPTOTIC SOLUTION OF THE FOKKER-PLANCK EQUATION

The problem of the collisional relaxation of a fast test charge moving through a gas of field electrons and ions has been described by the asymptotic form of the Fokker-Planck equation, and an analytic solution has been obtained. The treatment has been carried out for test and field particle distributions both of which are anisotropic in velocity space. It has been found that anisotropies in the field particle distributions make small contributions to the relaxation in the asymptotic region. Simple expressions have been obtained for the time development of the test particle velocity distribution. The results are used to study the production of a second peak in the velocity distribution function as a result of relaxation.

#### G. COHERENT AND INCOHERENT SCATTERING OF MICROWAVES BY PLASMAS

More careful measurements than reported before have been carried out on the radiation scattered at  $90^\circ$  to the primary beam in the plasma scattering experiment. The relative intensity of radiation scattered on to off-resonance has been found to be typically 50:1 to 100:1. The off-resonance intensity in equivalent black body temperature corresponds to  $\sim 30$  to  $50^\circ\text{K}$  temperature change. Studies have also continued on radiation scattered incoherently in the forward direction. Sidebands separated by 28 and 56 Mc/sec from the carrier have been detected with relative power levels of sideband to carrier differing by 130 db. This corresponds to a phase modulation of  $10^{-8}$  radian.

## H. COLLIDING PLASMAS

The colliding plasma experiment has been put into operation. The apparatus consists of two opposing coaxial plasma guns (cf. LAMS-2529, p.41) connected by a solenoidal magnetic guide field. The ends of the solenoid are coplanar with the muzzles of the guns, so that the plasma is required to penetrate along the axis of the strong solenoidal field. The phenomena observed in the experiment may be conveniently divided into two categories: (1) The properties of the faster plasma component ( $\sim 10^8$  cm/sec); and (2) The properties of the slower component ( $\sim 10^7$  cm/sec).

### The Fast Component

It has been previously reported that accelerated plasmas of the type considered here are filtered in translational energy and  $\beta$  by the process of penetrating along the axis of a magnetic mirror field. In particular, the fastest plasma component is little influenced by the mirror, and penetrates with  $\beta$  of the order of unity. The intersection of the fast plasmas results in a doubling of the diamagnetic signal observed with one gun alone, and, with deuterium loading of the guns, in a neutron pulse of duration equal to the transit time of the intersecting beams. The yield is in agreement with the collision of plasma streams at the previously established density ( $\sim 10^{14}$  per  $\text{cm}^3$ ) and translational velocity ( $\sim 10$  kev). Apparently, there is no collective interaction of the fast plasma component.

### The Slow Component

The diamagnetic signal associated with the slow component ( $\sim 10^7$  cm/sec) of the accelerated plasma was previously observed to vanish on the far side of the rise in a stepped magnetic field. This situation obtains in the present experiment for the simple solenoidal field, i.e., with a single gun, only a very weak diamagnetic signal associated with the slow component is observed 100 cm from the gun muzzle. Upon the collision of the opposed plasmas, there is a greatly enhanced diamagnetism ( $\sim 20$  times) of the slow plasma. These results imply that some part of the slow plasma

component in fact penetrates the field, but with negligible diamagnetism; that is, the motion is almost entirely along the field lines. The Coulomb collision cross section of the slower, more dense plasma is adequate to explain the transfer of the translational energy to transverse energy, and the resulting diamagnetic signal. The resulting plasma has a density of  $\sim 10^{16}$  per  $\text{cm}^3$ , with a mean kinetic temperature of  $\sim 100$  ev.

The neutron yield, the diamagnetic signal of the fast plasma component, and the plasma area have been measured as a function of the strength of the guide magnetic field for a fixed set of plasma gun parameters (14 kv on the gun capacitor banks and 1  $\text{cm}^3$ -atm of deuterium in each plenum). The neutron yield is assumed to be due to the collision of the plasma beams, and the diamagnetic signal is a measure of the flux excluded from the plasma. The plasma area is determined by a  $B_z$  probe to be  $\sim 50 \text{ cm}^2$ , independent of the strength of the guide field. When these data are combined with the experimental values of the velocity of the fast plasma, the time duration of the neutron pulse, and the injected plasma density, the transverse ion temperature  $kT_{\perp}$  (the electron temperature is assumed to be much less than the ion temperature) and  $\beta$  may be inferred from the following relations:

$$Y_n = N^2 \sigma / \alpha,$$

where  $Y_n$  = neutron yield,  $N$  = number of particles entering the guide field from each gun,  $\sigma$  = d-d cross section for beams colliding with relative energy 40 kev, and  $\alpha$  = plasma area,

$$n = 2N / \ell \alpha,$$

where  $n$  = plasma density in particles per  $\text{cm}^3$  and  $\ell$  = length of plasma (from neutron time duration,  $\ell = 100 \text{ cm}$ ).

$$nkT_{\perp} = \frac{2A}{\alpha} \frac{B_0 \Delta B}{8\pi} + \left( \frac{2A}{\alpha} - \frac{A^2}{\alpha^2} \right) \frac{(\Delta B)^2}{8\pi},$$

where  $A$  = area of flux conserving surface,  $B_0$  = strength of guide magnetic field, and  $\Delta B$  = change in field strength external to the plasma,

and

$$\beta = 8\pi nkT_i / (B_0 + \Delta B)^2.$$

The results of this analysis are shown in Fig. 7. The fact that  $kT_i$  is constant, independent of  $B_z$  whereas  $\beta$  is a sharply diminishing function with  $B_z$ , indicates that the simple picture of the penetration of a magnetic field by  $\beta = 1$  plasma does not apply to this experiment.

The number of particles entering the guide field decreases for  $B_z > 7$  kgauss, and is in agreement with the independent observation that as  $B_z$  increases, increasing numbers of neutrons are produced along its length. These neutrons presumably originate by the bombardment of plasma stopped by the solenoidal field with material which follows it. The neutrons produced at the ends of the solenoid occur earlier in time than the neutrons originating in the collision of the deuterium plasmas from the opposed guns, and are also produced by a single gun.

#### I. PENETRATION OF PLASMA INTO A TRANSVERSE MAGNETIC FIELD

As a preliminary to the  $\vec{E} \times \vec{B}$  acceleration experiment the penetration of the plasma from a coaxial gun into a transverse magnetic field has been studied. The capacitor bank of the gun (cf. LAMS-2529, p. 40) consists of three 20-kv Tobe capacitors, switched by means of ignitrons.

A chromel-alumel thermocouple soldered to a 1.5-mil copper sheet (16 mm x 8 mm) was used to detect plasma at a distance of 34 cm from the gun muzzle. Thermocouple data were taken with the gun injecting plasma in a transverse magnetic field of  $\sim 2.3$  kgauss. The gun muzzle was located  $\sim 10$  cm outside the end of a pair of long rectangular coils (130 cm x 30 cm) in a Helmholtz arrangement. The coil, which contained a long evacuated glass tube coaxial with the plasma gun, was energized with a 4 msec pulse from a 60 mf, 3 kv bank. The apparatus is shown in Fig. 8. It appears that the magnetic field deflects the plasma upwards from its zero-field trajectory. The field orientation is such that  $v_{in} \times B$  is down ( $v_{in}$  = injection velocity)

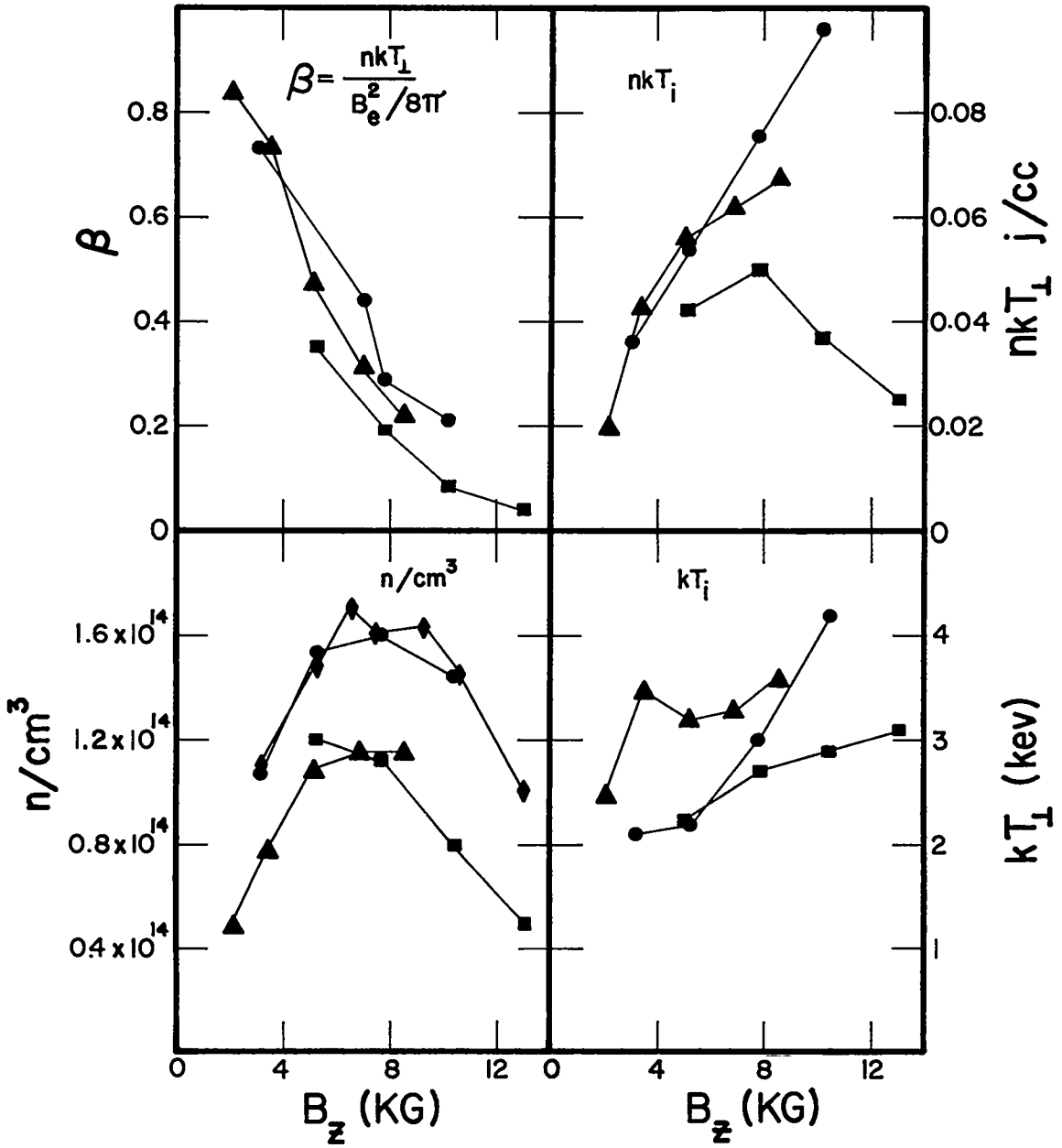


Fig. 7. Analysis of colliding plasma experiment

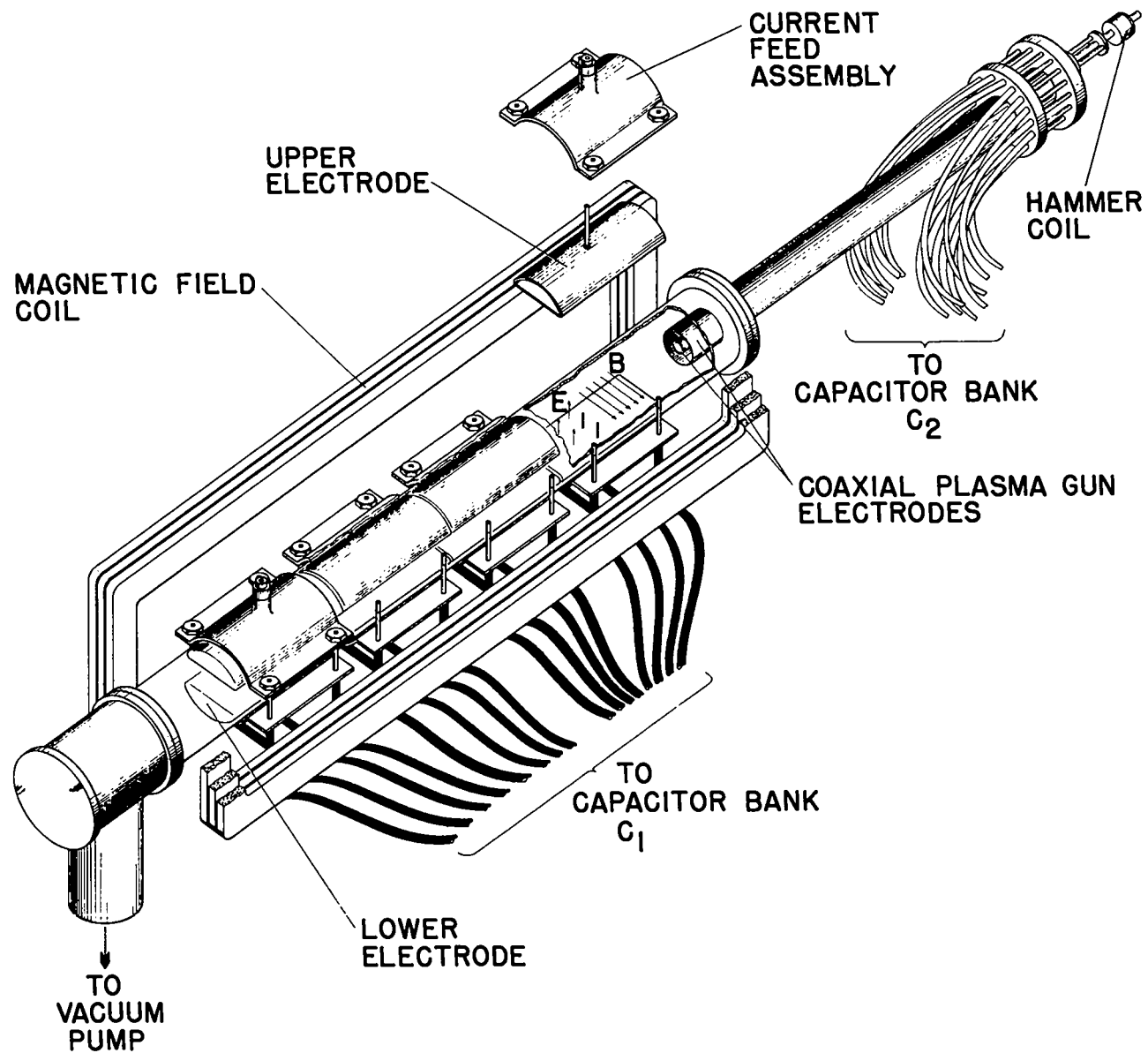


Fig. 8. Apparatus for study of penetration of plasma into a transverse magnetic field

so that the plasma is deflected in the same direction that injected electrons would be.

A magnetic probe was inserted in place of the thermocouple. It was found that the signals were diamagnetic (opposed the applied field) and were asymmetric in the same direction as indicated by the thermocouple. When the applied magnetic field was reversed, it was found that the location of the maximum diamagnetic signal shifted downwards indicating a plasma deflection in the opposite direction.

Since this plasma ( $\beta \approx 0.1$ ) is observed to penetrate the transverse field, an attempt was made to observe the polarization electric field which must be present for such a penetration. Conductors were placed at the probe ports located at positions 15 cm and 45 cm along the tube. The conductors were brought in from both sides of the plasma to positions  $\pm 5$  cm on either side of the tube axis. Thus one probe measured the voltage across 10 cm of plasma at the 15 cm position and the other at 45 cm. In order to correlate the observed voltage with the velocity of the plasma, an average velocity was obtained by observing the difference in arrival times of the voltage signals at the two probe positions. Table II records some results of voltage probe measurements. The last two columns give the comparison of E/B at peak signal and the average velocity for different magnetic fields and gun voltage delay.

TABLE II  
Voltage Probe Measurements

<u>Gun Voltage Delay</u>	<u>B</u>	<u>Peak Voltage</u>	<u>E/B cm/sec</u>	<u>Velocity cm/sec</u>
350 $\mu$ sec	830	1200	20	75
350	830	3000	50	75
350	1100	6500	60	50-75
350	2000	10000	50	40
350	2500	9000	30	35
450	2000	4300	20	25
450	1300	3750	30	25

(The coaxial gun was operated at 13 kv with a gas load of 0.6 cm<sup>3</sup>-atm of deuterium).

## J. SCYLLA III

Scylla III has been operated with a capacitor bank energy  $W$  of 180 kjoule, as well as with the 90 kjoule bank discussed in the last quarterly report (IAMS-2529, p. 38). Compression coils of the following lengths have been used: 10.6 (Scylla I coil-, 16.6, 18.7, 24.2, and 26.8 cm.

The plasma was photographed with the NRL model NLC streak camera used in previous work and also with a Kerr-cell camera at shutter speeds of 0.1 and 1  $\mu$ sec.

The accompanying photographs show the rotating structure described briefly in IAMS-2529, as well as its correlation in time with the applied magnetic field and the neutron emission.

Figure 9 depicts a violent instability developing in the 10.6 cm coil with  $W = 90$  kjoule and a maximum applied field of 104 kgauss. It should be noted that the neutron yield, instead of continuing to rise smoothly, is interrupted and becomes asymmetric about maximum magnetic field.

Figure 10 shows the effect of lengthening the coil to 16.6 cm with the same bank energy and a maximum magnetic field of 98 kgauss. The structure is now a smooth rotation of an elliptical plasma. The neutron yield is symmetric about the maximum magnetic field.

In Fig. 11 the bank energy was 180 kjoule, corresponding to 120 kgauss in the 18.7 cm coil. Here the neutron trace in (d) is asymmetric. Time scale: 1  $\mu$ sec/division.

Figure 12 represents the case  $W = 180$  kjoule and a coil length of 26.8 cm;  $B_{\max} = 103$  kgauss. The Kerr-cell photographs (0.1  $\mu$ sec exposure) of (b) and (c) are synchronized with the streak photographs and show the development of the elliptical cross section of the plasma. The neutron trace (e) is symmetric. Time scale 0.5  $\mu$ sec/division.

The longest stability time before onset of rotational structure is about 3  $\mu$ sec. The growth rate of the instability is about 10 times longer than the fastest predicted for the flute instability driven by the bending of the lines of the magnetic mirror. The parameters of the present experiment are such that

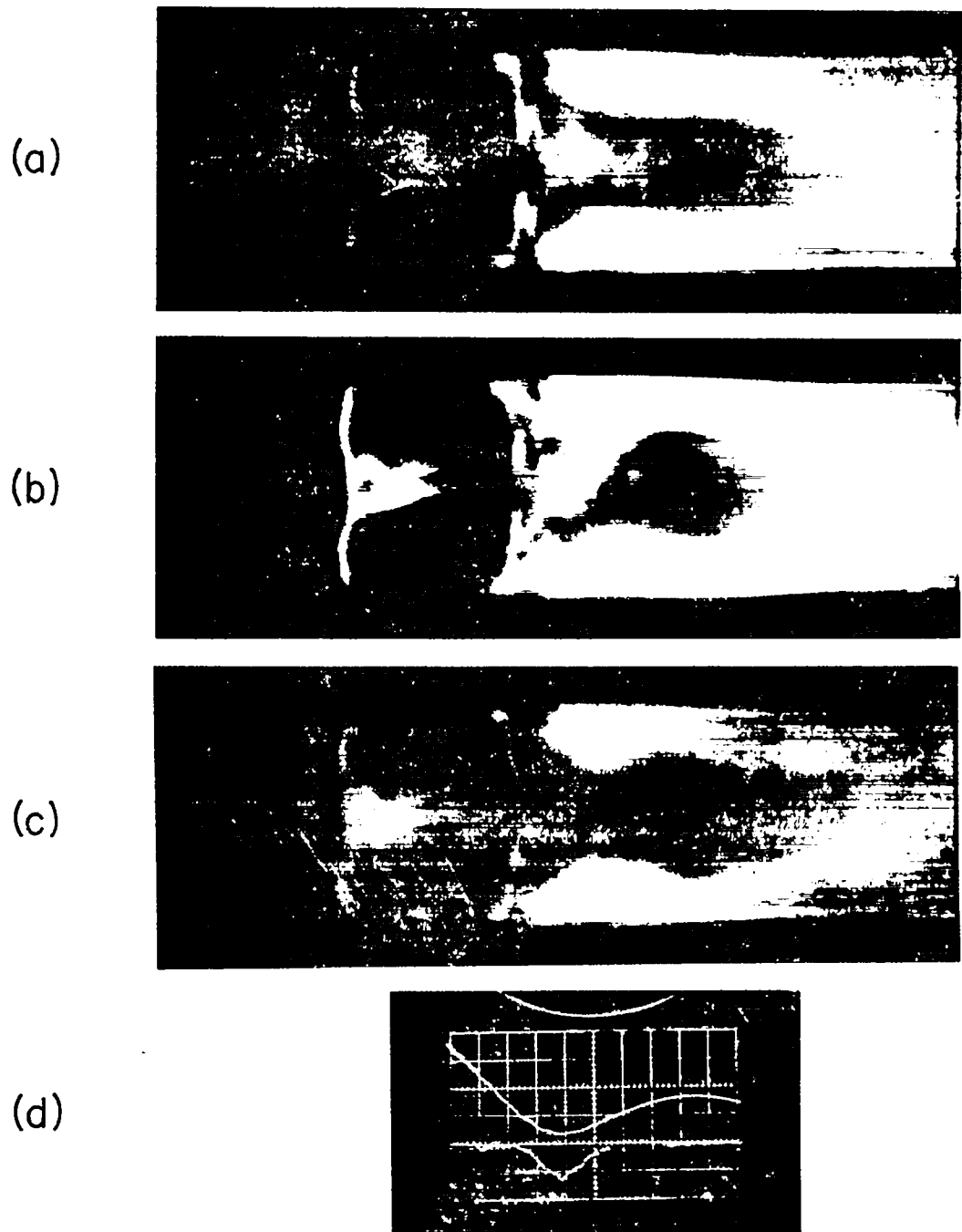


Fig. 9. Scylla III discharge: coil length 10.6 cm; capacitor bank energy 90 kjoule; maximum field  $10^4$  kgauss

(a)



(b)



(c)



(d)

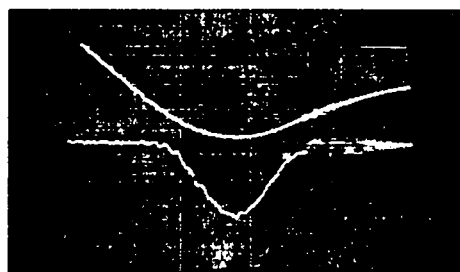


Fig. 10. Scylla III discharge: coil length 16.6 cm; capacitor bank energy 90 kjoule; maximum field 98 kgauss

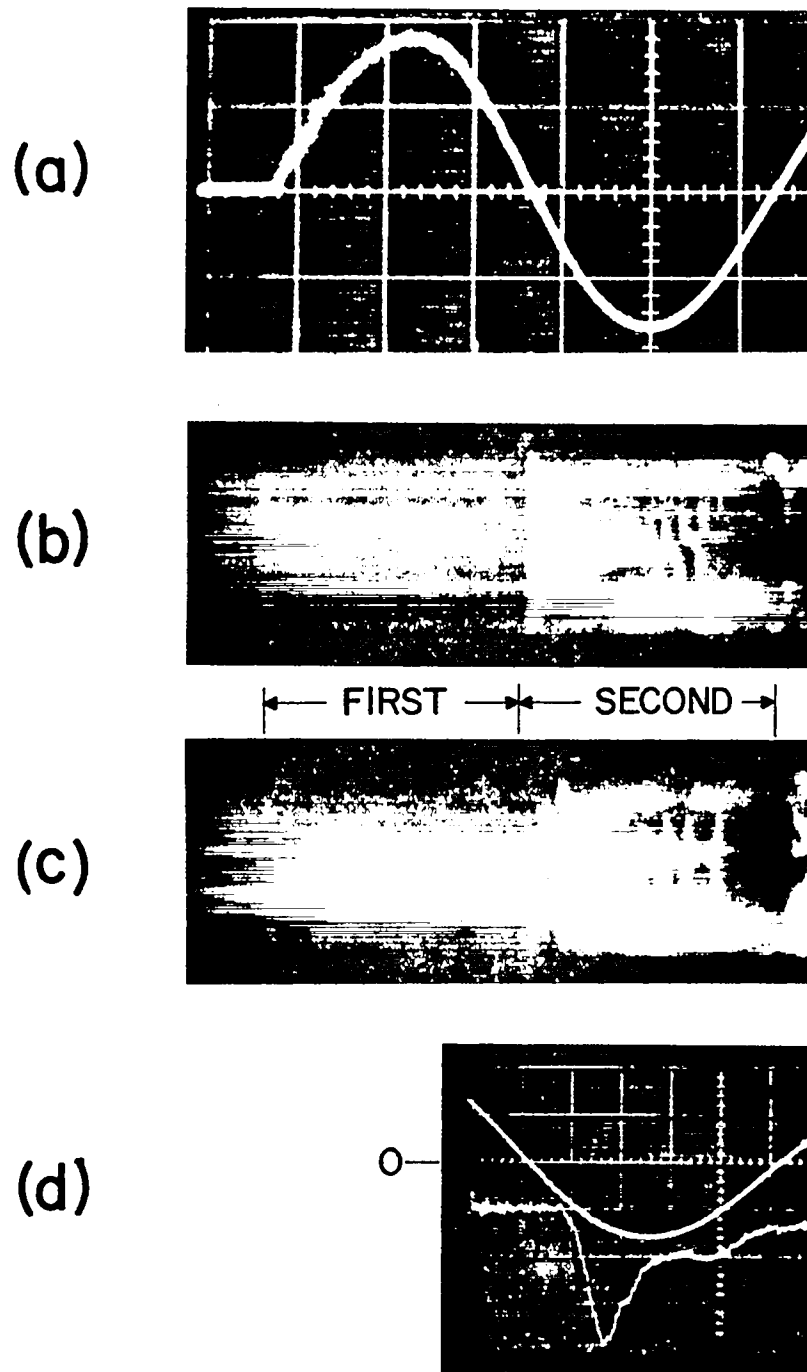


Fig. 11. Scylla III discharge: coil length 18.7 cm; capacitor bank energy 180 kjoule; maximum field 120 kgauss

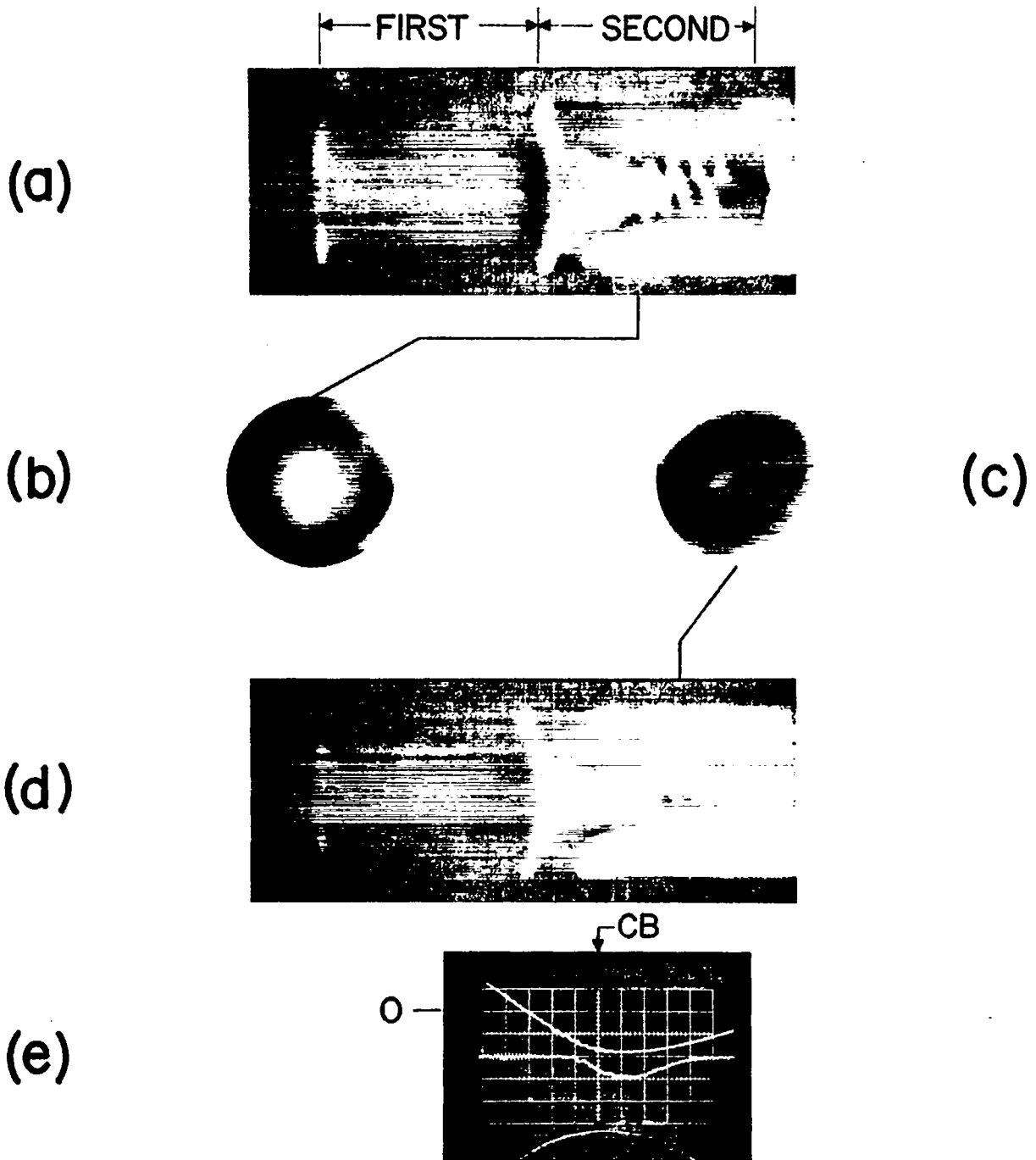


Fig. 12. Scylla III discharge: coil length 26.8 cm; capacitor bank energy 180 kjoule; maximum field 103 kgauss

the effect of finite ion Larmor radius, as predicted by Rosenbluth, et al., (private communication) should be apparent. This effect is to slow down the rate of flute growth.

#### K. X-RAY SPECTROSCOPY IN SCYLLA I

Boron trifluoride has been added as a trace impurity to the Scylla I discharge and several lines of F VIII and F IX have been observed. The line positions agree with predicted wavelengths to 0.1%. The helium-like lines of Al XII and Si XIII were remeasured and striking disagreements were found between observed wavelengths and those for the resonance series predicted from the lines occurring at longer wavelengths. It is probable that the observed lines are satellites similar to those previously reported in Ne IX, Na X, Mg XI. Another possibility, x-ray fluorescence radiation from the beryl crystal which contains both Si and Al, has been ruled out because the wavelengths observed are not good fits to tabulated x-ray lines.

#### L. X-RAY LINE BROADENING EXPERIMENTS IN SCYLLA I

##### Theory

For high-temperature, laboratory plasmas the dominant spectral line broadening mechanism in the soft x-ray region is the Doppler effect (thermal or turbulent velocity) distribution. Even the first order Stark effect for one electron ion is small in comparison. The reasons for this markedly different state of affairs compared to that in the optical region is that Doppler broadening is linear in wave length whereas Stark broadening is independent of frequency on an energy scale and therefore decreases as the square of the wavelength.

The relative magnitudes of the three major sources of line broadening (thermal, pressure, and natural) are illustrated by the computed full widths at half maximum intensity for the Lyman  $\gamma$  line of O VIII (15 A) at an ion temperature of 1 keV and in a deuterium plasma of density  $6 \times 10^{16}$  per  $\text{cm}^3$ .

$$\Delta\lambda_{\text{Doppler}} = 9 \times 10^{-3} \text{ \AA}$$

$$\Delta\lambda_{\text{pressure}} = 3.6 \times 10^{-6} \text{ \AA}$$

$$\Delta\lambda_{\text{natural}} = 6.3 \times 10^{-7} \text{ \AA}$$

### Experiment

The original x-ray spectrometer work (LAMS-2464, 2488, pps. 25, 29) which was intended primarily to explore the continuum, indicated numerous line radiations and showed that O VIII Lyman  $\gamma$  was broader than would be anticipated for  $kT = 1.3$  keV. The resolution limit set by the 11-min angular acceptance of the Soller slits ( $\sim 4 \times 10^{-3}$  \AA at 15 \AA and  $\sim 4 \times 10^{-2}$  \AA at 1.5 \AA) was insufficient to measure breadths of other lines at lower wavelengths.

New Soller slits of less than 3-min angular acceptance were built. If this were the new limiting instrumental resolution the observed line widths would be sufficiently greater to give quite accurate true widths. However, the diffraction pattern of the beryl crystal itself, which was measured to be 40 sec of arc for  $\text{CuK}\alpha$  radiation, increases rapidly with wavelength and is the new limiting factor at wavelengths greater than 7 \AA. It thus turns out that the instrumental profile gives a large contribution to the observed line profiles. The instrumental profile was assumed to approximate a Lorentz (or dispersion) shape because of the following observation. The Zn  $L\alpha$  line measured 7-min half width for a double arm-crystal rock and 4 min for a detector arm rock, consistent with the fold of two dispersion shapes and the known width of 3 min for this line.

The best data on Scylla were obtained for the Ne IX  $1s^2 \ ^1S_0 - 1s2p \ ^1P_1$  line. Its profile, together with the intercombination line  $1s^2 \ ^1S_0 - 1s2p \ ^3P_1$  and a longer wavelength satellite are shown in Fig. 13. Each point is an average of at least two discharges. The two curves, differing only in intensity, show reproducibility on different days.

To reduce these data to a temperature, it is assumed that the true line shape is Gaussian (Doppler broadening) and the observed half width

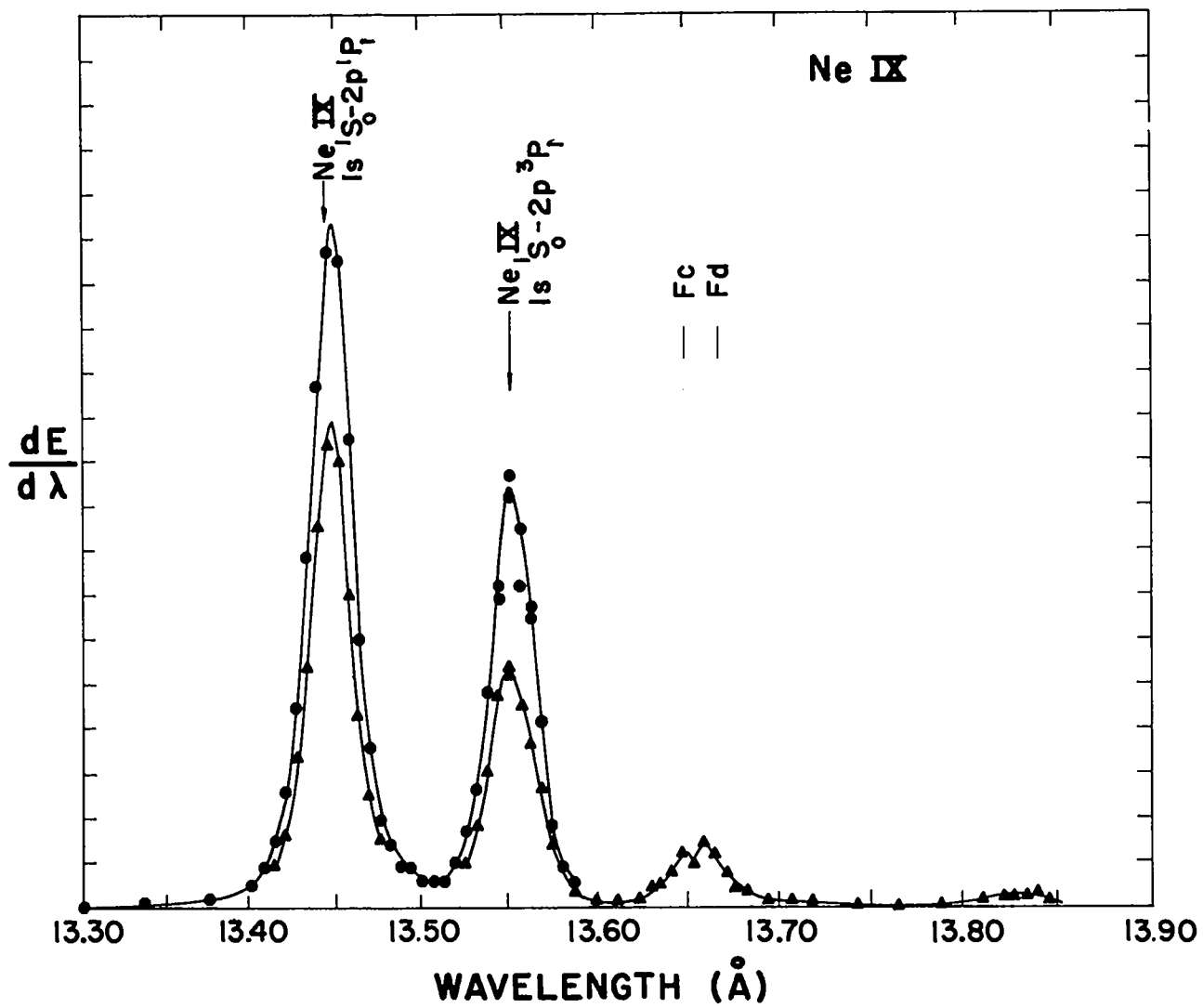


Fig. 13. Neon IX lines from Scylla I

the result of folding this Gaussian with the known dispersion shape of the instrument. The observed resultant is therefore a Voigt function and the Gaussian contribution to the total width can be derived from tabulations of Voigt functions.

Finally, 
$$\Delta\lambda = 2d \cos \theta \Delta\theta$$

and 
$$kT = 8(\ln 2) \frac{Mc^2}{\lambda^2} (\Delta\lambda)^2.$$

### Results

a) For Ne IX  $1s^2 \ ^1S_0 - 1s2p \ ^1P_1$ :  $kT = 8.4$  kev.

Independent determinations for the  $3p$  and  $5p$  neon lines gave respectively  $kT = 10.5$  and  $13.5$ . However, by changing the assumed instrumental half width from  $3$  min to  $4$  min and from  $2-1/2$  min to  $4-1/2$  min, respectively, these values are reduced to  $kT = 8.4$  in agreement with the  $2p$  value. This illustrates the sensitivity of the results to the poorly known instrumental resolution.

Ne Lyman  $\alpha$  :  $kT = 7.7 \pm 2$  kev

b) Oxygen Lyman  $\gamma$  :  $kT \sim 6.5$  kev

This is a wide line, in a region of large instrumental profile determined only by a large extrapolation.

c) F VIII  $1s^2 \ ^1S_0 - 1s4p \ ^1P_1$  :  $kT \sim 5.4$  kev

This line is so close to the neon  $2p$  line (and on the long wavelength side) that regardless of the true instrumental profile the conclusion that the effective  $T$  is less than that for neon is certain. (However, the average neutron yield in the neon case was 50% greater).

d) The temperatures of the wall impurities Na and Mg seemed, if anything, to be higher, and not lower, than the temperatures for the contaminants added in gaseous form prior to the discharge.

e) For a change of the main gas from deuterium to hydrogen and then to helium, the half width of neon IX  $1s^2 \ ^1S_0 - 1s3p \ ^1P_1$  remained constant to within the experimental sensitivity.

f) For the neon contaminant alone at  $5 \mu$  pressure (the same partial pressure as above) the line breadth increased.

g) For a discharge in neon alone at a pressure of  $90 \mu$  the x-ray monitor signal decreased by about four orders of magnitude.

### Conclusions

The effective temperatures of impurities are substantially greater than the deuterium ion temperature. The experiment is not good enough to establish whether a simple relationship exists between effective temperature and mass or total charge. A higher effective temperature could be explained by a small "turbulent velocity" which is more effective in producing large widths for large masses or a truly higher temperature reflecting a higher efficiency of the heating mechanism (as apparently exists for deuterium ions relative to electrons) since the times available are somewhat marginal for inter-ion equilibration. It is not presently possible to infer deuterium temperature from impurity line broadening.

### M. SCYLLA IV

The design for Scylla IV has begun. This experiment is the next step in the program for the study of plasma heating by fast magnetic compression. The system is intended to provide a fast-rising initial compression field from a primary capacitor bank, followed by a more slowly rising (power crowbar) field applied from a secondary bank. The 50-kv primary bank is being designed with sufficiently low internal inductance to give the same coil voltage (40 kv) as that previously attained in Scylla I and III with a 100-kv bank.

The system will use four capacitor banks; the primary bank will store 560 kjoules at 50 kv, the secondary power crowbar bank will store 3 megajoules at 20 kv, the bias field bank will store 290 kjoules at 10 kv and the preionization bank will store 30 kjoules at 60 kv. The secondary bank will be three racks of Zeus modified to have a low-source inductance. The bias field bank will also be a part of Zeus.

The primary bank will consist of 448, 2- $\mu$ f, 50-kv low inductance capacitors. Each capacitor will have its own 4-element spark gap mounted to it. Each gap will have six low-inductance coaxial cables connecting it to a collector plate of a parallel plate transmission line. This primary bank will be mounted on a platform which will be located in front of three of the Zeus racks. The transmission line will be below the primary bank, positioned to minimize the cable lengths.

The preionization bank will also be on the platform. It will consist of 17, 0.8- $\mu$ f, 120-kv capacitors, each with its own spark gap and 10 load cables. This bank will be initially charged to 60 kv but will subsequently be transiently charged by the primary bank to over 100 kv.

The firing sequence will be as follows: The bias bank will be fired and the current will rise to a maximum in about 500  $\mu$ sec. Then the preionization bank will be fired and produce 1.9 Ma with an 0.85  $\mu$ sec quarter period. The primary bank will then be fired and produce 10 Ma with an 11- $\mu$ sec quarter period. The secondary bank will act as a power crowbar to deliver 20 Ma with a 22- $\mu$ sec quarter period. These currents will then be allowed to oscillate.

The transmission line must accommodate 2348 cables in the header section and sustain the magnetic forces generated by the 30 Ma peak current. The line will have a rectangular section 15 ft wide by 18 ft long and a 3 ft long section that tapers down to 40 in. in order to bolt onto a 1-meter compression coil.

A Scylla IV Steering Committee has been formed to guide the design of this experiment. Design responsibilities have been assigned to various members of all three LASL Sherwood groups. The schedule indicates a firing date for Scylla IV in the spring of 1962.

#### N. ZEUS

The low-inductance cabled shelf described in the last quarterly report generated interest in using Zeus as a power crowbar in a new Scylla experiment. During the ensuing discussions it was discovered that parts of

Zeus should be charged negative. Previously Zeus has always been positive. The negative polarity immediately required a change in the geometry of the switch header.

The resulting coaxial header, shown in Fig. 14, has several convenient features. Being coaxial it has an inherent low inductance. The stacked rings are simpler to build and easy to assemble and maintain. The cathodes of the ignitrons are common and cooled with a single cooling coil on the cathode ring. Since the bank is charged negative, one ignitron can be used to trigger all 16 load ignitrons. The trigger energy is supplied by the capacitor bank and so no firing set capacitor is required. The geometry of the assembly allows the trigger ignitron and the ignitor current limiting resistors to be conveniently mounted in the center of the header. The lower cables go to the capacitors and the upper cables go to the load. The current return, which is a shell that is clamped between upper and lower rings, is not shown. A polyethylene sheet insulates the center ring from the shell.

The header was tested at 20 kv carrying 1 Ma ringing at 12 kc. The shelf inductance measured 0.026  $\mu$ h with a resistance of 0.9 milliohm. During the testing at 20 kv, two capacitors failed during the charge cycle at voltages above 19 kv. In both cases the protect circuit previously described operated as predicted and protected the dead capacitors by firing the load ignitron and delivering most of the stored energy into the load.

One difficulty with the cable scheme is that all the capacitor cables must have the same inductance. This can be accomplished by making all cables the same length but storage for the excess cable in the capacitor rack presents a problem. A number of small inductors were designed and built to make up various equivalent lengths of cable, thereby saving 300 ft of cable per shelf. Each coil was potted in epoxy to allow it to sustain the magnetic pressure created in it while carrying large currents. The coils operated satisfactorily carrying 20 ka with the bank charged to 20 kv.

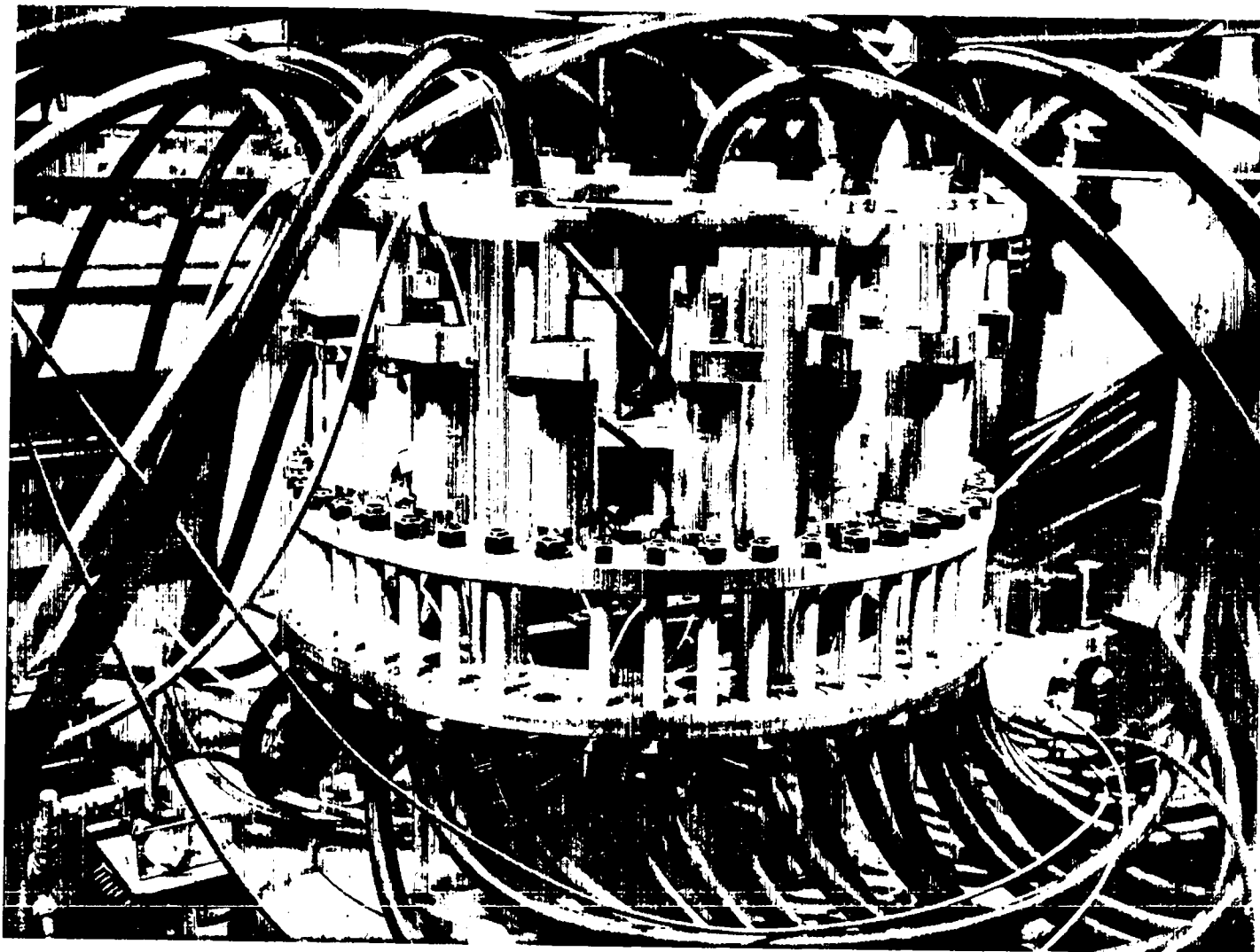


Fig. 14. New coaxial switch header for Zeus